Molecular Dynamics Simulations of Ibuprofen Binding to Aβ Peptides

E. Prabhu Raman,[†] Takako Takeda,[‡] and Dmitri K. Klimov[‡*]
[†]Department of Pharmaceutical Sciences, School of Pharmacy, University of Maryland, Baltimore, Maryland; and [‡]Department of Bioinformatics and Computational Biology, George Mason University, Manassas, Virginia

ABSTRACT Using replica exchange molecular dynamics simulations and the implicit solvent model we probed binding of ibuprofen to $A\beta_{10-40}$ monomers and amyloid fibrils. We found that the concave (CV) fibril edge has significantly higher binding affinity for ibuprofen than the convex edge. Furthermore, binding of ibuprofen to Aβ monomers, as compared to fibrils, results in a smaller free energy gain. The difference in binding free energies is likely to be related to the presence of the groove on the CV fibril edge, in which ibuprofen tends to accumulate. The confinement effect of the groove promotes the formation of large low-energy ibuprofen clusters, which rarely occur on the surface of Aβ monomers. These observations led us to suggest that the ibuprofen binding mechanism for Aβ fibrils is different from that for monomers. In general, ibuprofen shows a preference to bind to those regions of Aβ monomers (amino terminal) and fibrils (the CV edge) that are also the primary aggregation interfaces. Based on our findings and on available experimental data, we propose a rationale for the ibuprofen antiaggregation effect.

INTRODUCTION

Aggregation of polypeptide chains and formation of amyloid fibrils are associated with the development of a number of disorders, including Alzheimer's, Parkinson's, type II diabetes, and Creutzfeldt-Jakob disease (1). Amyloid assembly generally proceeds through a complex sequence of structural transitions, which starts with the oligomerization of monomeric chains and eventually leads to the formation of amyloid fibrils (2). Experimental data indicate that oligomers, even as small as dimers, appear to be the primary cytotoxic species (3–6). Because amyloid fibrils are reservoirs of monomers, they may play an important role in the dynamic equilibrium of soluble oligomeric species (7–9). The hallmark of fibril internal organization is an extensive β-sheet structure (10–14). Backbone hydrogen bonds and a host of side-chain interactions lend considerable stability to amyloid fibrils against dissociation (15).

Aggregation of Aβ peptides (Fig. 1, *a–c*), which are the natural products of cellular proteolysis, is linked to Alzheimer's disease (AD). The most abundant Aβ species are 40-mer peptides ($A\beta_{1-40}$). The structure of fibril protofilament for these peptides has been recently derived from solid-state NMR experiments (12) (Fig. 1 *c*). This structure reveals parallel in-registry β-sheets formed by Aβ monomers (11,13).

Given the apparently critical role of Aβ peptides in AD pathogenesis, it is important to find molecular agents that make it possible to control Aβ aggregation. One of the promising candidates is the nonsteroidal antiinflammatory drug ibuprofen (16). Biomedical studies suggest that treatment with ibuprofen reduces the amount of Aβ deposits and alleviates memory deficits in mice models (17,18). Ibuprofen intake also correlates with a decrease in the amount of Aβ oligomers in mice brain tissues (18). A prophylactic long-term use of ibuprofen appears to reduce the risk of AD (19), but the effectiveness of this drug against preexisting AD cases is unclear (20). Several recent experimental studies have investigated the molecular aspects of interactions between Aβ and ibuprofen. Binding of ibuprofen to Aβ fibrils has been demonstrated when the ligand/peptide stoichiometric ratio approximates or exceeds 1 (21,22). Experimental in vitro studies have shown that ibuprofen reduces accumulation of Aβ fibrils by apparently interfering with fibril elongation (23). Furthermore, ibuprofen demonstrates an ability to at least partially dissociate preformed Aβ fibrils (21,23).

Despite progress in experimental observations, there are still many questions about Aβ-ibuprofen interactions on a molecular level. For example, 1), where are the ibuprofen binding sites in Aβ peptides and what are the physicochemical factors controlling ibuprofen binding? 2), Are there differences in binding affinity among the different Aβ species, such as monomers or fibrils? 3), Does ibuprofen binding induce changes in Aβ peptide structure? Answering these questions will be important to our understanding of the mechanism of Aβ fibril dissociation induced by ibuprofen and may aid in designing new antiaggregation agents.

All-atom computer simulations, such as molecular dynamics (MD), are well suited to provide molecular-level details of Aβ-ibuprofen interactions (24). In recent years, MD has been used to map the pathways of fibril growth (25–30), to investigate the conformational ensembles of amyloidogenic peptides (31–34), and to assess the energetics of fibril structures (35–38). However, molecular simulations of amyloidogenic peptides coincubated with ligands are still relatively rare. Binding of the fluorescence dye thioflavin T (ThT) to the fibrils formed by Aβ fragments, $A\beta_{16-22}$, has been probed using all-atom MD (39). Two ThT binding sites were identified, one in the hydrophobic groove on the fibril side and another on the fibril edge. From MD simulations, the

Submitted June 17, 2009, and accepted for publication July 22, 2009.

*Correspondence: dklimov@gmu.edu

Editor: Ruth Nussinov.

0006-3495/09/10/2070/10 $2.00

doi: 10.1016/j.bpj.2009.07.032

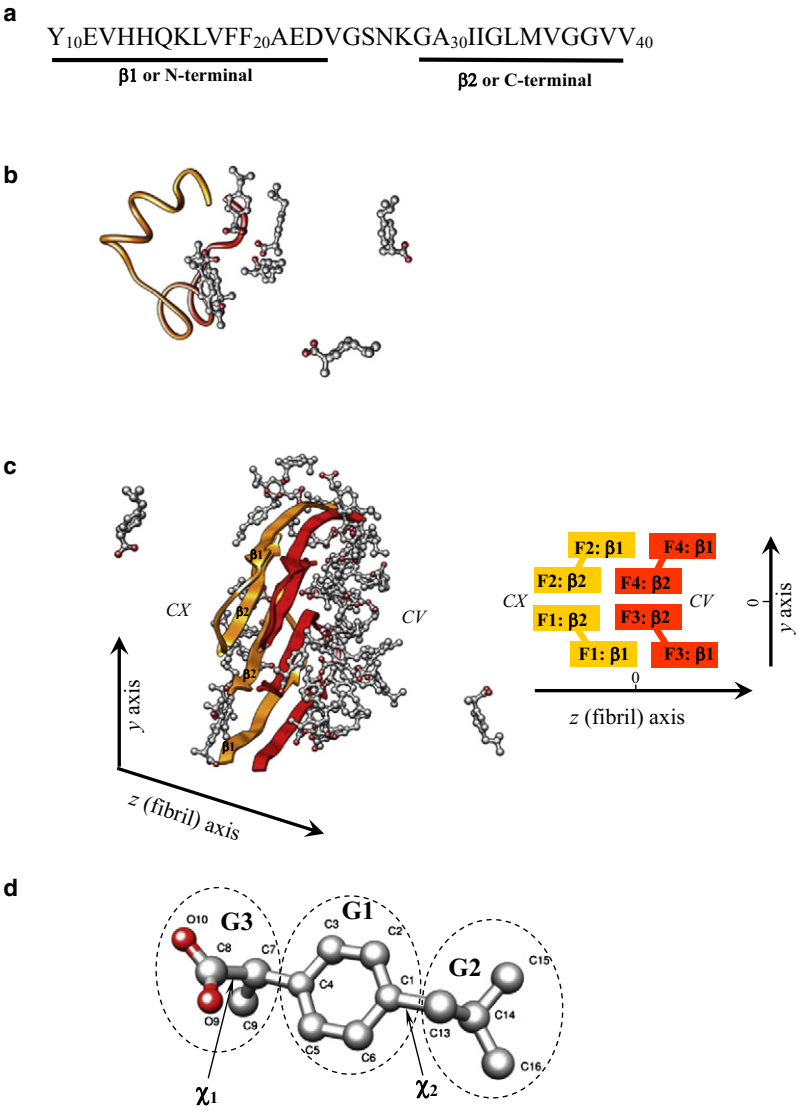

FIGURE 1 (*a*) Sequence of A$\beta_{10–40}$ monomer and the allocation of the N- and C-terminals (also referred to as β1 and β2 strands). (*b*) Representative snapshot of A$\beta_{10–40}$ monomer with bound ibuprofen molecules. The N- and C-terminals are shown in red and orange, respectively. The N-terminal has a higher binding affinity than the C-terminal. (*c*) Cartoon representation of A$\beta_{10–40}$ fibril fragment formed by four peptides, F1 and F2 (*orange*), and F3 and F4 (*red*), with bound ibuprofen molecules. The fibril protofilament consists of four laminated in-registry β-sheets formed by the β1 and β2 strands in the Aβ peptide portrayed in *a*. The stagger of inner β2 sheets with respect to β1 sheets results in the appearance of two distinct fibril edges, a concave (CV) and a convex (CX) edge. On the CV edge, indented β2 sheets form a groove. The CX and CV edges are formed by the peptides F1 and F2, and F3 and F4, respectively. Compared to the CX edge, the CV edge has a higher binding affinity for ibuprofen. As a result, ligands tend to localize on the CV edge, forming large clusters in the groove. (*d*) An ibuprofen molecule showing the atoms with their notations, which are explicitly represented in the CHARMM19 force field (see the Supporting Material for ibuprofen parameterization). Also shown are the structural groups G1–G3 (*dashed circles*) and dihedral angles χ_1 and χ_2.

binding energetics for ThT was also computed. More recently, binding of tricyclic planar ligands (9,10-anthraquinone and anthracene) to fibril forming Aβ fragments A$\beta_{14–20}$ was investigated using MD (40). The results showed that 9,10-anthraquinone interferes with the formation of interstrand hydrogen bonds and reduces the accumulation of ordered aggregates. However, to the best of our knowledge, MD studies of ibuprofen binding to Aβ have not been performed.

In this article, we address the three questions posed above using the atomistic implicit solvent model and replica exchange molecular dynamics (REMD) (41). By conducting separate simulations, we investigate the binding of ibuprofen molecules to Aβ monomers and to experimentally determined structures of Aβ fibrils. These two systems have been selected because monomers and fibrils represent the initial and final products in the Aβ amyloidogenic pathway. Extensive sampling in a wide range of temperatures allowed us to compute thermally weighted distributions of ibuprofen molecules in the vicinity of Aβ monomers and fibrils and to compare their binding free energies. On the basis of these results, we propose an antiaggregation mechanism of ibuprofen.

METHODS

Molecular dynamics simulations

Simulations of Aβ peptides and ibuprofen (Fig. 1) were performed using the CHARMM MD program (42) and the atomistic force field CHARMM19 coupled with the solvent-accessible surface area (SASA) implicit solvent model (43). A detailed description of this model, as well as its applicability and testing, can be found in our previous studies (44,45). In particular, the CHARMM19+SASA force field has been shown to reproduce well the experimental distribution of chemical shifts for C_α and C_β atoms (45). Parameterization of ibuprofen (Fig. 1 *d*) was performed consistent with the CHARMM19 force field, SASA solvation parameters, and taking into account the similarity of ibuprofen structure to that of Leu, Phe, and Asp side chains. Because the pKa value for ibuprofen is 4.5, the polar group

COO was assumed to be deprotonated and, according to the SASA implicit solvent model, was set neutral to prevent excessive stability of salt bridges (43). The complete list of ibuprofen force-field parameters is given in the Supporting Material. Testing of ibuprofen parameterization is reported below.

We consider two simulation systems: 1), A$\beta_{10–40}$ monomer interacting with $N_{ibu} = 10$ ibuprofen molecules; and 2), the fibril fragment formed by four A$\beta_{10–40}$ peptides interacting with $N_{ibu} = 40$ ibuprofen molecules. In both systems, we used N-terminal truncated Aβ peptides as a model of the full-length A$\beta_{1–40}$ (34). Further description of the simulation systems is provided in the Supporting Material and in our previous studies (34,44). The Aβ peptide/ibuprofen concentration ratio is 1:10, which is only slightly higher than that used experimentally (21,23). Throughout this article, the peptides in Fig. 1 *c* are referred to as fibrils.

Replica exchange simulations

Conformational sampling was performed using REMD (41). This method makes it possible to achieve exhaustive sampling of rugged free-energy landscapes and has been applied to study protein folding and aggregation (26,30,46–49). The details of REMD implementation and its convergence are discussed in the Supporting Material.

Computation of structural probes

The intrapeptide interactions and those between Aβ peptides and ibuprofen were probed by computing the number of side-chain contacts and hydrogen bonds (HBs). A side-chain contact was considered formed if the distance between the centers of mass of side chains is <6.5 Å (50). Computation of contacts formed by ibuprofen molecules is described in the Supporting Material.

Intrapeptide backbone HBs between NH and CO groups were assigned according to Kabsch and Sander (51). The same definition was applied to detect HBs between hydrophilic groups G3 in ibuprofen and peptide backbone NH groups. Secondary structure in Aβ peptides was assigned based on the distribution of backbone dihedral angles (ϕ and ψ). Specific details concerning the definitions of β-strand and helix states can be found in a previous publication (45). Throughout this article, angular brackets $<\ldots>$ imply thermodynamic averages. Unless stated otherwise, all quantities related to ibuprofen represent the averages over all ibuprofen molecules. The distributions of states produced by REMD were analyzed using the multiple histogram method (52).

Testing force field parameterization of ibuprofen

Recently, a conformational analysis of ibuprofen was performed using density functional theory and verified by optical vibrational spectroscopy (53). From this analysis, the distributions of two dihedral angles, χ_1 and χ_2 (Fig. 1 *d*), became available, which offers us an opportunity of testing CHARMM19 ibuprofen parameterization. The testing results can be found in the Supporting Material.

RESULTS

Guided by the allocation of secondary structure in experimental fibril structure (12) (Fig. 1, *a* and *c*), we distinguish two sequence regions in A$\beta_{10–40}$: the N-terminal (NT, residues 10–23), corresponding to the first fibril β-strand, β1, and the C-terminal (CT, residues 29–39), corresponding to the second fibril β-strand, β2.

Binding of ibuprofen to Aβ monomers

As described in Methods, we used REMD and the implicit solvent model to probe the interactions of ibuprofen molecules with A$\beta_{10–40}$ monomers (Fig. 1 *b*). We first computed the thermal probability of an ibuprofen molecule binding to Aβ (P_b) as a function of temperature. Fig. 2 shows that at $T \lesssim 310$ K, $P_b(T) > 0.5$, indicating that ibuprofen bound states are thermodynamically preferred. Consequently, the binding temperature (T_b) is assumed to be ~310 K. Because it is close to physiological temperature, the thermodynamic quantities for Aβ monomer are reported at T_b. The total number of ibuprofen molecules bound to Aβ at 310 K is $<L> = N_{ibu}P_b \approx 4.9$ (Fig. 2, *inset*). The inset also shows the number of ibuprofen molecules, $<L_h(T)>$, bound to Aβ by forming hydrophobic interactions. Because at 310 K $<L_h> \approx 3.3 = 0.67<L>$, we conclude that about two-thirds of ligands utilize hydrophobic interactions for binding.

Fig. 3 shows the numbers of contacts with ibuprofen formed by individual side chains of residues i in Aβ monomer, $<C_l(i)>$. Although there are significant variations in $<C_l(i)>$ between neighboring residues, one can discern a tendency for the N-terminal to form a large number of contacts with ibuprofen. Indeed, on average, the N-terminal forms $<C_l(\mathrm{NT})> \approx 10.9$ contacts with ibuprofen (or 0.8/residue). In contrast, the number of contacts between the C-terminal and ibuprofen is $<C_l(\mathrm{CT})> \approx 4.8$ (or 0.4/residue). Therefore, the N-terminal forms about twice as many interactions with ibuprofen compared to the C-terminal. The total number of side-chain contacts with ibuprofen, $<C_l>$, is ~18.4. Because the number of ligands bound to Aβ, $<L>$, is ~4.9, each ligand interacts with about $<C_l>/<L> \approx 3.8$ amino acids. These calculations suggest that as a rule, each bound ibuprofen molecule forms contacts with multiple amino acids.

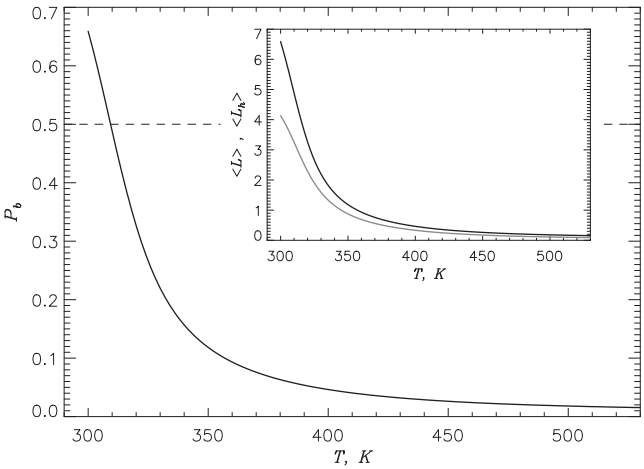

FIGURE 2 Probability of an ibuprofen molecule binding to an Aβ monomer as a function of temperature ($P_b(T)$). The dashed line marks $P_b = 0.5$. (*Inset*) Temperature dependence of the average number of ligands bound to Aβ monomer, $<L_h>$, via hydrophobic interactions (*gray curve*) compared with the total number of bound ibuprofen molecules, $<L(T)>$ (*black curve*). At temperatures <310 K, the ibuprofen bound state is thermodynamically preferred.

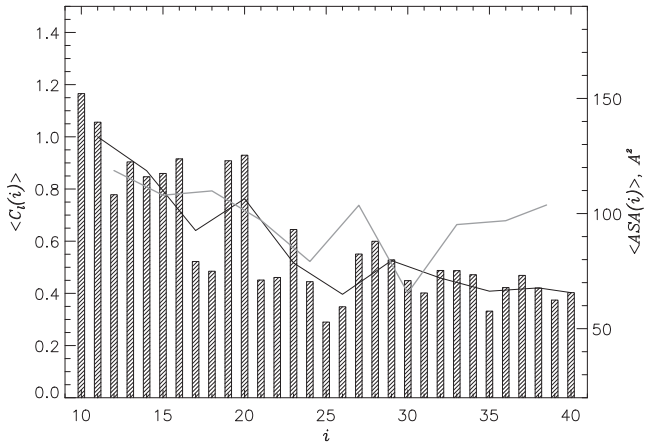

FIGURE 3 Number of contacts with ibuprofen, $<C_l(i)>$, formed by side chains of residues i in Aβ monomer. The black line represents $<C_l(i)>$ smoothed with the sliding window of three residues, and the gray line shows accessible surface area $<\mathrm{ASA}(i)>$ of amino acids i (also smoothed with the sliding window of three residues). The plot implies that ibuprofen primarily binds to the N-terminal of Aβ monomers. The data are computed at 310 K. To compute ASA, the probe radius was set to 3.2 Å, which corresponds to the average radius of gyration of ibuprofen molecules.

It is of interest to compare the contributions of side-chain interactions and backbone HBs to binding energetics. Fig. S3 in the Supporting Material shows the number of HBs, $<N_{\mathrm{hb}}(i)>$, formed between the backbone NH groups of amino acids i and the oxygen atoms in the ibuprofen group G3 (Fig. 1 *d*). Except for the few N-terminal residues $<N_{\mathrm{hb}}(i)> < 0.05$. From Fig. S3, we determine that the total number of HBs formed between ibuprofen and peptide backbone is $<N_{\mathrm{hb}}> \approx 1.6$. Because $<N_{\mathrm{hb}}>$ is more than 10 times smaller than the number of contacts between ibuprofen and side chains, $<C_l>$, the contribution of HBs to binding is small.

Next, we evaluate the impact of ibuprofen binding on the conformational ensemble of Aβ monomer. To this end, we compare the fractions of β-strand, $<S>$, and helix, $<H>$, structure formed by $A\beta_{10-40}$ monomers in water and in ibuprofen solution. The distribution of $A\beta_{10-40}$ secondary structure in water has been investigated in previous studies (34,45). Fig. S4 in the Supporting Material shows the ibuprofen-induced changes in β-strand ($<\Delta S(i)>$) and helix ($<\Delta H(i)>$) structures formed by residues i. These plots reveal small but systemic conversion of helix into strand structure. The average change in the fraction of residues in β-strand conformations is $<\Delta S> = <S_{\mathrm{ibu}}> - <S_{\mathrm{w}}> \approx 0.06$, where $<S_{\mathrm{W}}>$ (~0.16) and $<S_{\mathrm{ibu}}>$ (~0.21) are the β-strand fractions in water and ibuprofen solution, respectively. The helix fraction reveals a small decrease ($<\Delta H> \approx -0.04$), from $<H_{\mathrm{W}}> \approx 0.38$ in water to $<H_{\mathrm{ibu}}> \approx 0.34$ in ibuprofen solution. However, the fraction of random coil structure remains unchanged within computational error (0.46 in water versus 0.45 in ibuprofen solution). Therefore, the impact of ibuprofen binding on secondary structure of Aβ monomer appears to be weak and the peptide retains mostly random coil conformations augmented by significant helix and strand contents. In the Supporting Material, we also show that ibuprofen causes minor changes in the radius of gyration of Aβ monomer (Fig. S5).

Binding of ibuprofen to Aβ fibrils

To explore binding of ibuprofen to $A\beta_{10-40}$ fibrils (Fig. 1 *c*), we utilized a strategy similar to that used for $A\beta_{10-40}$ monomers. Using REMD, we computed the temperature dependence of the binding probability, $P_{\mathrm{b}}(T)$, for the ibuprofen molecule. Fig. 4 shows that the midpoint of $P_{\mathrm{b}}(T)$ corresponds approximately to $T = 362$ K, which is identified as the binding temperature, T_{b}. Therefore, bound ibuprofen states are stable at $T < T_{\mathrm{b}}$. It is important to note that, compared to $A\beta_{10-40}$ monomers, the fibril T_{b} is higher by ~50 K. Below, the binding properties of ibuprofen are reported at 330 K, the closest temperature to physiological conditions, for which REMD sampling is available.

The binding probability, P_{b}, does not distinguish peptides or edges in the fibril. To map the distribution of ibuprofen molecules on the fibril surface, we considered two fibril edges, the convex (CX) and concave (CV), formed by the peptides F1 and F2, and F3 and F4, respectively (Fig. 1 *c*). The numbers of ligand molecules bound to the CX and CV edges as a function of temperature are presented in the inset to Fig. 4. This plot indicates that at $T < T_{\mathrm{b}}$, there is a preference for ibuprofen molecules to bind to the CV edge. For example, at 330 K, the number of ligands bound to the CV is $<L(\mathrm{CV})> \approx 22.1$, whereas for the CX edge it is $<L(\mathrm{CX})> \approx 15.2$. The inset also shows the numbers of

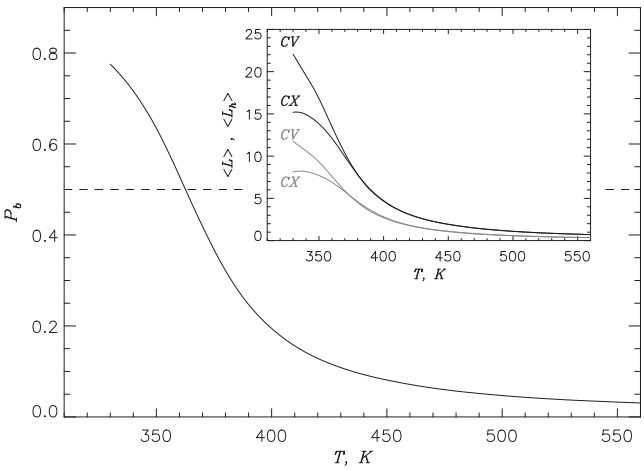

FIGURE 4 Probability of ibuprofen molecules binding to Aβ fibrils as a function of temperature, $P_{\mathrm{b}}(T)$. The dashed line marks $P_{\mathrm{b}} = 0.5$. (*Inset*) Numbers of ibuprofen molecules, $<L(\mathrm{CV})>$ (*black line*) and $<L(\mathrm{CX})>$ (*gray line*), bound to the CV and CX edges, respectively, versus temperature. The numbers of ligands bound to the CV ($<L_{\mathrm{h}}(\mathrm{CV})>$; *gray line*) and CX ($<L_{\mathrm{h}}(\mathrm{CX})>$; *gray line*) edges via hydrophobic interactions are also plotted. At temperatures $\lesssim 362$ K, the ibuprofen bound state is thermodynamically preferred, and most ligands are found on the CV edge.

ibuprofen molecules, $<L_h(CV)>$ and $<L_h(CX)>$, bound to the CV and CX fibril edges via hydrophobic interactions. Although significantly smaller, $<L_h(CV)>$ and $<L_h(CX)>$ follow the same temperature dependence as $<L(CV)>$ and $<L(CX)>$. At 330 K, $<L_h(CV)>$ and $<L_h(CX)>$ are ~11.8 and ~8.1, respectively. Thus, approximately half of all ligands are bound to the fibril through hydrophobic interactions.

To get further insight into the binding mechanism, we computed the number of contacts $<C_l>$ formed between ligands and the side chains on fibril edges. On average, the CX and CV edges form $<C_l(CX)> \approx 47.0$ and $<C_l(CV)> \approx 69.8$ contacts with ibuprofen. Taking into account that the CX (CV) edge binds ~15.2 (22.1) ligands, we surmise that a bound ibuprofen molecule interacts with about three amino acids at once. We also obtained the numbers of HBs formed between the CX and CV peptide backbones and ibuprofen, $<N_{lhb}(CX)>$ and $<N_{lhb}(CV)>$. At 330 K, $<N_{lhb}(CX)> \approx 6.2$, whereas $<N_{lhb}(CV)> \approx 5.5$. Therefore, the number of side-chain contacts exceeds the number of HBs eightfold on the CX edge and 13-fold on the CV edge. As in the case of Aβ monomer, binding of ibuprofen to Aβ fibril is mainly driven by side-chain interactions.

The findings reported above suggest that the CV edge has a higher affinity for ibuprofen than does the CX edge. This result can be illustrated by computing the spatial distribution of ligands, $P(z)$, along the fibril axis, z (Fig. 5 *a*). It follows from this distribution that the fractions of ligands bound to the CV and CX edges are 0.55 and 0.29, respectively. The probability of binding to the fibril side (Fig. 5 *a*) is very low (0.03) and is ~30 times smaller than the combined probability of edge binding (see Discussion).

It is also important to map the spatial distributions of ibuprofen on two fibril edges. To this end, we considered two distributions, $P_{CX}(y)$ and $P_{CV}(y)$, which are computed for the CX and CV edges along the y axis perpendicular to the fibril axis (Fig. 1 *c*). Fig. 5 *b* demonstrates that $P_{CX}(y)$ and $P_{CV}(y)$ have different profiles, reflecting distinct geometries of the edges. Because the β2 strands are protruding on the CX edge, $P_{CX}(y)$ shows two poorly defined maxima at $+10$ Å and -10 Å, approximately corresponding to the gaps between the β1 and β2 sheets (Fig. 1 *c*). In contrast, a single maximum of large amplitude is observed in $P_{CV}(y)$, corresponding to the location of the groove formed by indented β2 sheets on the CV edge. Therefore, upon binding to the CV edge, ibuprofen tends to localize within the groove.

It is instructive to directly visualize the observations made based on $P_{CV}(y)$ and $P_{CX}(y)$ in Fig. 5 *b*. To this end, we computed the fibril surface area accessible to ibuprofen and mapped onto this surface the location of amino acids

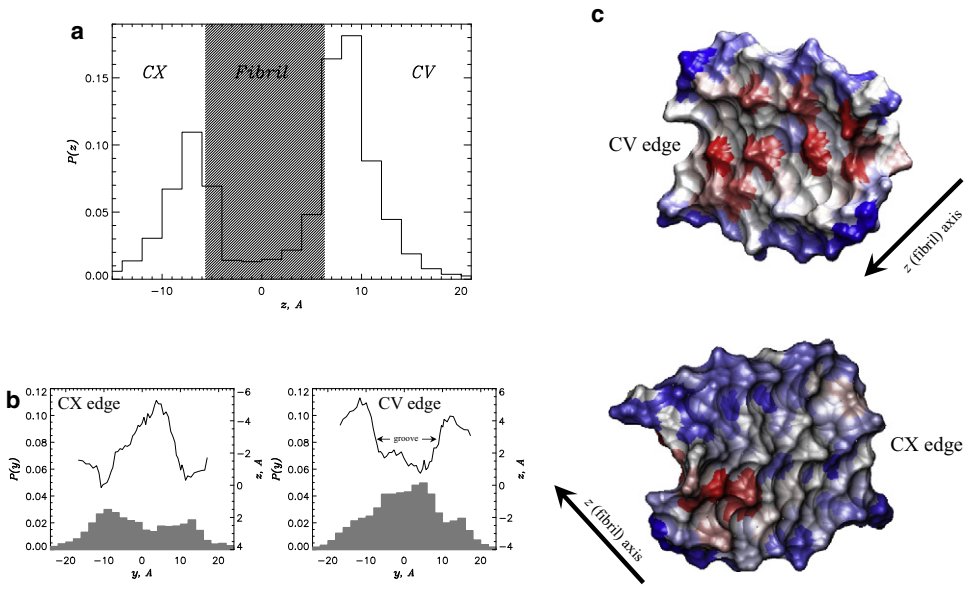

FIGURE 5 (*a*) Probability distribution for the position of ibuprofen center of mass along the fibril axis z, $P(z)$. To estimate the probabilities of binding, we assume that the ligand is located on the CX edge if -15 Å $< z < -3$ Å, on the CV edge if 3 Å $< z <$ 17 Å, and on the fibril side if -3 Å $< z <$ 3 Å. The shaded area approximately marks the maximum extent of fibril fragment. (*b*) Probability distributions, $P(y)$, (*shaded area*) for the center-of-mass position of ibuprofen along the y axis perpendicular to the fibril axis. The left and right panels are computed for the CX ($z < 0$) and CV ($z > 0$) edges, respectively. The plots also show the smoothed projections of the edge surfaces on the yz plane (*black lines*, see also Fig. 1 *c*). The edge surface is represented by the side-chain centers of mass. (*c*) The surfaces of the CV and CX edges accessible to ibuprofen computed using a probe radius of 3.2 Å (ibuprofen radius of gyration). The surfaces of residues i in peptides k are color-coded according to the number of side-chain contacts $<C_l(i;k)>$ they form with ibuprofen at 330 K: red, gray, and blue correspond to large, medium, and small $<C_l(i;k)>$ values, respectively. (Although the fibril pictured in *c* and used in *a* and *b* corresponds to the energy-minimized structure, it serves as a good representation of the thermally weighted fibril surface. For example, the correlation between the water ASA(i) for the energy-minimized structure and that computed at 330 K is >0.95). The probability distributions in *a*–*c*, computed at 330 K show that ibuprofen primarily binds to the CV edge and localizes within the groove on its surface.

that have a high probability of interaction with ligands. It can be seen from Fig. 5 *c* that the amino acids showing a large number of interactions with ibuprofen are those in the CV groove (or on its rim), and especially those protruding from the groove surface. To determine ibuprofen binding sites, we operationally selected amino acids i in peptides k = F3,F4 for which the number of contacts with ibuprofen $<C_l(i;k)>$ is no less than 70% of the maximum (i.e., $<C_l(i;k)> \geq 0.7 \max_{i,k}\{<C_l(i;k)>\}$). With this definition, ibuprofen binding sites include Gln^{15}(F3), Gly^{29}(F3), Ile^{31}(F3), Met^{35}(F3), Val^{39}(F3), Glu^{11}(F4), Gln^{15}(F4), Phe^{19}(F4), and Val^{40}(F4). The list includes both hydrophobic and hydrophilic amino acids and appears to imply that ibuprofen binding is mainly driven by fibril surface geometry rather than by physicochemical properties of individual residues. Using the same definition, we found that the CX edge binding sites involve only three amino acids: Ser^{26}(F1), Ala^{30}(F1), and Ile^{32}(F1) (Fig. 5 *c*). (Setting the net charge of ibuprofen to zero in the CHARMM19 force field might affect its binding to the fibril. However, it is unlikely that the neglect of ibuprofen charge qualitatively changes the binding to the fibril, because only 1 of 12 amino acids identified as primary binding sites is charged.)

Binding free energy

There are some indications from experimental studies that as a ligand, ibuprofen selectively ''recognizes'' Aβ fibrils among other structural species (see Discussion) (54). To check this possibility, we used REMD to compute the free energies of ibuprofen binding to Aβ monomers and fibrils. Fig. 6 displays the free energies of ibuprofen molecules, $F(r_b)$, as a function of the distance, r_b, between the ligand and the surface of the monomer or fibril. The two free-energy profiles are qualitatively similar and show a single minimum at $r_{b,0} \approx 5$ Å. From Fig. 6, the binding free energy can be defined as $\Delta F_b = F(r_{b,0}) - F(r_b > 20)$. Using this definition, we determine that $\Delta F_b{}^m$ for the monomer and $\Delta F_b{}^f$ for the fibril are $-3.7RT$ and $-5.9RT$, respectively. This result implies that fibril-bound ibuprofen states are more stable (by ~2.2RT) than monomer-bound states.

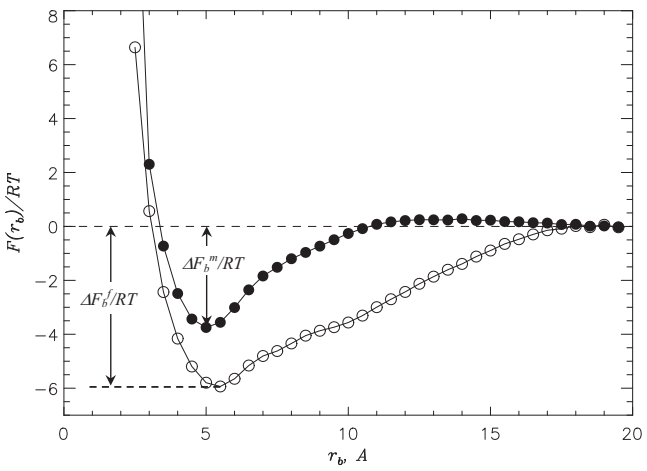

FIGURE 6 Free energy of an ibuprofen molecule, $F(r_b)$, as a function of the distance, r_b, between the ligand and the surface of Aβ monomers (*solid circles*) or fibrils (*open circles*). Free-energy profiles, $F(r_b)$, reveal that binding to fibrils is thermodynamically preferred. The free energy, $F(r_b)$, is obtained at 330 K using all binding states of all the ligands that are populated at this temperature; the free energy at $r_b > 20$ Å is set to zero.

DISCUSSION

In this study, we used REMD and an atomistic model to investigate ibuprofen binding to Aβ monomers and fibrils. Consistent with experiments (21,23), we observed that at low enough temperatures, ibuprofen binds to Aβ species and that binding to Aβ fibrils is thermodynamically preferred over binding to monomers. By analyzing the distribution of ligands on the surface of Aβ monomers and fibrils, we located the putative binding sites. These observations raise two questions: 1), What are the physicochemical factors that control ibuprofen binding? and 2), Can we use the results of REMD simulations to explain the antiaggregation effect observed experimentally for ibuprofen?

Cooperativity of ibuprofen binding to Aβ fibril

To provide some tentative answers to the questions above, we analyzed the distribution of clusters formed by bound ligands on the surface of Aβ fibrils at 330 K. A bound cluster is defined as an isolated group of ibuprofen molecules bound to the fibril edge that do not form contacts with other bound ligands (see Methods). The size of a cluster, S_c, is given by the number of ibuprofen molecules included. Using REMD, we computed the distributions of bound ligands, $<L(S_c)>$, where $<L(S_c)>$ is the thermally averaged number of molecules in a cluster of size S_c. Of particular interest is the distribution $<L(S_c)>$ for the CV fibril edge (Fig. 1 *c*). This distribution (shown in Fig. S6 *a*) is bimodal, featuring two maxima at $S_c = 1$ and 22. If we assume that cooperatively bound ligands comprise the clusters with $S_c > 6$, then their number is $<L_{cl}(CV)> \approx 17.8 \approx \phi<L(CV)>$, where $<L(CV)> \approx 22.1$ is the total number of ibuprofen molecules bound to the CV edge and $\phi \approx 0.81$. The distribution $<L(S_c)>$ for the CX edge is qualitatively different. Fig. S6 *b* reveals one maximum in $<L(S_c)>$ at $S_c = 1$ and the distribution is generally skewed toward small S_c (e.g., $<L_{cl}(CX)>$ is only ~6.0). Consequently, ϕ for the CX edge is 0.40.

Further analysis suggests that the formation of large clusters on the CV edge reduces the average effective energy, E_{eff}, of the simulation system, which includes potential and solvation energies. Specifically, when all ligands bound to the CV edge are organized into large clusters ($S_c > 6$), E_{eff} is $\Delta E_{eff} \approx 19$ kcal/mol lower than the energy of the states, which have only small clusters ($S_c \leq 6$). It is of interest

that similar computations for the CX edge show no decrease in E_{eff} upon formation of large ibuprofen clusters.

We have reported that the number of ligands bound to the CV edge, $<L(CV)>$, exceeds that on the CX edge, $<L(CX)>$, by a factor of 1.5. The analysis presented above suggests a rationale for the preference of ibuprofen molecules for binding to the CV edge. The distributions $<L(S_c)>$ demonstrate that large clusters of bound ligands frequently appear on the CV edge, but are relatively rare on the CX edge. According to Fig. 5, *b* and *c*, most ibuprofen molecules bound to the CV are localized within the groove. It is then reasonable to suggest that this geometrical feature of Aβ fibrils facilitates the formation of large ibuprofen clusters due to a ''confinement'' effect of the groove. As shown above, the formation of large clusters tends to reduce the energy of the system. Because the CX edge has no groove, such an effect is not observed, and the affinity of the CX edge is low compared to that of the CV edge. The conclusion that the binding surface geometry determines ligand binding finds support in simulations of structurally modified fibril (Supporting Material). By eliminating the CV groove and enhancing the small grooves on the CX edge, the affinity of the ''new'' CX edge becomes as strong as the affinity of the ''wild-type'' CV edge (Fig. S7).

Therefore, the geometry of the binding surface appears to be more important for ibuprofen association with Aβ fibrils than specific sequence composition or accessible surface area (ASA). (We observed no correlation between the number of contacts ibuprofen forms with side chains, $<C_l(i;k)>$, and ibuprofen ASA of amino acid *i* in peptide *k*, $<ASA(i;k)>$.) This conclusion is supported by the mixture of residue types involved in ibuprofen binding sites. Furthermore, a relevant observation has been made in experiments on the ligand-induced dissociation of fibrils formed by Aβ and α-synuclein polypeptides (23,55). In these experiments, nine different antiaggregation ligands, including ibuprofen, were evaluated for their dissociation efficiency. It is intriguing that the order of their antiaggregation efficiency remains the same for both polypeptides, even though their sequence similarity is low (9%). This observation suggests that the sequence composition may not be the leading factor in ligand binding. It is important to note that the grooves on the fibril surface represent the primary binding sites for other ligands. For example, scanning tunneling microscopy experiments have shown that ThT dye is localized in the grooves formed on the surface of Aβ_{42} fibril-like aggregates (56). A similar conclusion has been reached in a recent MD study (39). These reports are consistent with our finding that the CV groove is a primary binding location for ibuprofen.

According to our REMD simulations, side-chain interactions with ibuprofen, rather than backbone HBs, play a major role in ligand binding to Aβ. According to the analysis of fibril (and monomer) binding, the number of side-chain contacts with ibuprofen exceeds the number of HBs between peptide backbone and the ligand ~10-fold.

Finally, it is instructive to comment on ibuprofen binding to the fibril sides. The small size of the fibril fragment we studied may artificially suppress the probability of fibril side binding. However, we believe that this limitation is not crucial, because it is the binding sites on the fibril edges that are apparently responsible for the ibuprofen antiaggregation effect. As discussed below, the edges appear to represent the fibril elongation interface.

Factors controlling ibuprofen binding to Aβ monomers

The distribution of ibuprofen molecules, $<L(S_c)>$, bound to Aβ monomer does not resemble that seen on the CV fibril edge, but is qualitatively similar to that on the CX edge (data not shown). For example, the fraction of ligands confined to large bound clusters, ϕ, is only 0.1, and the distribution, $<L(S_c)>$, is unimodal at 310 K. The absence of stable structural pockets or grooves in the monomer devoid of stable native fold is likely to disfavor the formation of large ligand clusters. This circumstance is expected to limit the free-energy gain that occurring upon ibuprofen binding to Aβ monomers relative to the fibrils. As demonstrated above, compared to binding to monomeric species, binding to Aβ fibrils is favored by ~2.2*RT*. Consequently, the binding temperature, T_b, for the fibril is ~50 K higher than for the Aβ monomer.

It is known from experimental studies that the molecular imaging probe FDDNP competes for the same Aβ binding sites as ibuprofen (21). Since FDDNP associates with Aβ fibrils with higher affinity than with other structural species (54), one can assume that similar structural selectivity exists for ibuprofen. These arguments are consistent with our simulations, which offer a molecular explanation for the selectivity of ibuprofen with respect to different structural Aβ species.

We have shown that there is a preference for ibuprofen to bind to the N-terminal of Aβ monomers. Analyzing the number of contacts between ibuprofen and amino acid side chains, $<C_l(i)>$, we found that the N-terminal forms about twice as many interactions with ibuprofen as does the C-terminal (Fig. 3). Because Aβ monomers do not have a stable native fold, the cooperativity arguments advanced above cannot explain this preference. However, a plausible explanation is provided by the ibuprofen ASA of residues. In Fig. 3, we plot the average $<ASA(i)>$ for residues *i* in Aβ monomers. It is seen that the N-terminal is more accessible for ligands than the C-terminal. From Fig. 3, we compute the total ASA of the N-terminal, $<ASA(NT)>$ to be ~1615 Å^2 (or 115 Å^2/residue). In contrast, the C-terminal ASA, $<ASA(CT)>$, is considerably smaller (~980 Å^2 or 89 Å^2/residue). This variation in ASA along the Aβ sequence is consistent with the change in $<C_l(i)>$. Therefore, the ASA of amino acids is a factor in binding ibuprofen to Aβ monomers, which is not the case for Aβ fibrils. Taken together, our

simulations suggest that the binding mechanisms for Aβ fibrils and monomers are different.

Plausible antiaggregation mechanism of ibuprofen

It is useful to consider the simulations of ibuprofen binding in the context of our previous studies of Aβ aggregation. We showed earlier that the primary aggregation interface in $A\beta_{10–40}$ dimers involves the N-terminal sequence (residues 10–23) (34,45). This sequence region forms about twice as many interpeptide side-chain contacts as the C-terminal. It is intriguing that the N-terminal in Aβ monomers also shows the highest affinity for binding ibuprofen (Fig. 3). It is also important that ibuprofen binding appears to have little impact on the conformational ensemble of Aβ monomers. Therefore, ibuprofen is likely to interfere directly with interpeptide interactions and destabilize the Aβ aggregation interface. The alternative antiaggregation mechanism, in which changes in Aβ structure make it less susceptible to aggregation, is not supported by our findings.

Our previous simulations showed that the N-terminal is also the primary aggregation interface in $A\beta_{10–40}$ fibril growth (44). Furthermore, the CV edge has ~10-fold higher affinity for binding incoming Aβ peptides than the CX edge (30,44). It is noteworthy that our current results show that ibuprofen preferentially binds to the CV edge and localizes within the CV groove. Therefore, one may suggest that upon binding to the CV edge, ibuprofen directly interferes with the deposition of incoming Aβ peptides by destabilizing peptide-fibril side-chain interactions.

The picture of the ibuprofen antiaggregation effect described above is consistent with some experimental observations. For example, it has been shown that ibuprofen reduces the number of Aβ oligomers in mouse brain tissues (18). Ibuprofen largely inhibits fibril assembly when coincubated with ''fresh'' (not fibrillized) Aβ peptides (21,23). Moreover, ibuprofen at a concentration of 50 μM completely blocks Aβ fibril elongation (23). Because amyloid fibrils grow via monomer addition to its edges (57–61), the fact that ibuprofen is capable of blocking fibril elongation indicates that it binds to the edges of the fibril. This conclusion is consistent with our computational findings (Fig. 5 *a*).

Finally, we compare the numbers of binding sites in Aβ fibrils mapped from experimental data and our simulations. It has been suggested that the molecular imaging probe FDDNP uses the same binding sites as ibuprofen (54). This observation raises the possibility of using FDDNP binding sites in lieu of ibuprofen binding sites. For FDDNP, two binding sites have been reported with high and low affinities (54). It is important to note that the number of binding sites/number of fibril peptides was estimated at ~3.5:10,000 (high affinity) and 7.1:10,000 (low affinity). A possible interpretation of these findings is that FDDNP (and ibuprofen) binds to the edges of Aβ fibrils, which have different affinities for incoming ligands. This interpretation would be in line with our in silico results described above.

CONCLUSIONS

Using REMD simulations and the implicit solvent model, we examined binding of ibuprofen to $A\beta_{10–40}$ monomers and fibrils. At sufficiently low temperatures, the bound ibuprofen states are thermodynamically stable. We found that the concave (CV) fibril edge reveals significantly higher affinity for ibuprofen binding than the convex (CX) edge. Binding of ibuprofen to Aβ monomers appears to depend on the exposure of amino acids to ligands and results in a smaller free-energy gain than binding to fibrils. The difference in binding free energies is apparently related to the presence of the groove on the CV fibril edge, in which bound ibuprofen tends to accumulate. The confinement effect produced by the groove promotes the formation of large low-energy ibuprofen clusters on the fibril surface. Due to the lack of stable fold, large ibuprofen clusters do not occur on the Aβ monomer surface. Therefore, binding mechanisms for Aβ monomers and fibrils appear to be different.

It is important to note that ibuprofen shows a preference to bind to those regions of Aβ monomers (N-terminal) and fibrils (the CV edge) that also represent the primary aggregation interfaces. Based on these findings and experimental data, we have suggested a rationale for the ibuprofen antiaggregation effect. Because $A\beta_{10–40}$ appears to be an adequate model for the $A\beta_{1–40}$ peptide (34), the results of our study should be applicable to full-length Aβ species.

SUPPORTING MATERIAL

Additional text, seven figures, and references are available at http://www.biophysj.org/biophysj/supplemental/S0006-3495(09)01288-0.

The content of this article is solely the responsibility of the authors and does not necessarily represent the official views of the National Institute on Aging or the National Institutes of Health. Fig. 1 was produced using the University of California at San Francisco Chimera package (62). The authors thank Prof. J. Harvey for providing the files with ibuprofen parameterization in the CHARMM22 force field (63). The authors declare no competing financial interests.

This work was supported by a grant from the National Institutes of Health National Institute on Aging (R01 AG028191).

REFERENCES

1. Selkoe, D. J. 2003. Folding proteins in fatal ways. *Nature*. 426:900–904.
2. Dobson, C. M. 2003. Protein folding and misfolding. *Nature*. 426:884–890.
3. Kayed, R., E. Head, J. L. Thompson, T. M. McIntire, S. C. Milton, et al. 2003. Common structure of soluble amyloid oligomers implies common mechanism of pathogenesis. *Science*. 300:486–489.
4. Haass, C., and D. J. Selkoe. 2007. Soluble protein oligomers in neurodegeneration: lessons from the Alzheimers amyloid β-peptide. *Nat. Rev. Mol. Cell Biol*. 8:101–112.

5. Pastor, M. T., N. Kümmerer, V. Schubert, A. Esteras-Chopo, C. G. Dotti, et al. 2008. Amyloid toxicity is independent of polypeptide sequence, length and chirality. *J. Mol. Biol.* 375:695–707.
6. Shankar, G. M., S. Li, T. H. Mehta, A. Garcia-Munoz, N. E. Shepardson, et al. 2008. Amyloid-β protein dimers isolated directly from Alzheimers brains impair synaptic plasticity and memory. *Nat. Med.* 14:837–842.
7. Murphy, R. M., and M. M. Pallitto. 2000. Probing the kinetics of β-amyloid self-association. *J. Struct. Biol.* 130:109–122.
8. Carulla, N., G. L. Caddy, D. R. Hall, J. Zurdo, M. Gair, et al. 2005. Molecular recycling within amyloid fibrils. *Nature*. 436:554–558.
9. Martins, I. C., I. Kuperstein, H. Wilkinson, E. Maes, M. Vanbrabant, et al. 2008. Lipids revert inert Aβ amyloid fibrils to neurotoxic protofibrils that affect learning in mice. *EMBO J.* 27:224–233.
10. Serpell, L. C. 2000. Alzheimer's amyloid fibrils: Structure and assembly. *Biochim. Biophys. Acta*. 1502:16–30.
11. Burkoth, T. S., T. Benzinger, V. Urban, D. M. Morgan, D. M. Gregory, et al. 2000. Structure of the β-Amyloid(10–35) fibril. *J. Am. Chem. Soc.* 122:7883–7889.
12. Petkova, A. T., W.-M. Yau, and R. Tycko. 2006. Experimental constraints on quaternary structure in Alzheimer's β-amyloid fibrils. *Biochemistry*. 45:498–512.
13. Luhrs, T., C. Ritter, M. Adrian, D. R. Loher, B. Bohrmann, et al. 2005. 3D structure of Alzheimers amyloid-β(1–42) fibrils. *Proc. Natl. Acad. Sci. USA*. 102:17342–17347.
14. Nelson, R., M. R. Sawaya, M. Balbirnie, A. O. Madsen, C. Riekel, et al. 2005. Structure of the cross-β spine of amyloid-like fibrils. *Nature*. 435:773–778.
15. Meersman, F., and C. M. Dobson. 2006. Probing the pressure-temperature stability of amyloid fibrils provides new insights into their molecular properties. *Biochim. Biophys. Acta*. 1764:452–460.
16. Xia, W. 2003. Amyloid inhibitors and Alzheimer's disease. *Curr. Opin. Investig. Drugs*. 4:55–59.
17. Heneka, M. T., M. Sastre, L. Dumitrescu-Ozimek, A. Hanke, I. Dewachter, et al. 2005. Acute treatment with the PPARγ agonist pioglitazone and ibuprofen reduces glial inflammation and Aβ_{1-42} levels in APPV717I transgenic mice. *Brain*. 128:1442–1453.
18. McKeea, A. C., I. Carrerasc, L. Hossainc, H. Ryua, W. L. Kleine, et al. 2008. Ibuprofen reduces Aβ, hyperphosphorylated τ and memory deficits in Alzheimer mice. *Brain Res.* 1207:225–236.
19. Akiyama, H., S. Barger, S. Barnum, B. Bradt, J. Bauer, et al. 2000. Inflammation and Alzheimer's disease. *Neurobiol. Aging*. 21:383–421.
20. Imbimbo, B. P. 2004. The potential role of non-steroidal anti-inflammatory drugs in treating Alzheimer's disease. *Expert Opin. Investig. Drugs*. 13:1469–1481.
21. Agdeppa, E. D., V. Kepe, A. Petric, N. Satyamurthy, J. Liu, et al. 2003. In vitro detection of (s)-naproxen and ibuprofen binding to plaques in the Alzheimer's brain using the positron emission tomography molecular imaging probe 2-(1-(6-[(2- [18F]fluoroethyl)(methyl)amino]-2-naphthyl)ethylidene) malononitrile. *Neuroscience*. 117:723–730.
22. Levine, H. 2005. Multiple ligand binding sites on Aβ_{1-40} fibrils. *Amyloid*. 12:5–14.
23. Hirohata, M., K. Ono, H. Naiki, and M. Yamada. 2005. Non-steroidal anti-inflammatory drugs have anti-amyloidogenic effects for Alzheimer's β-amyloid fibrils in vitro. *Neuropharmacology*. 49:1088–1099.
24. Ma, B., and R. Nussinov. 2006. Simulations as analytical tools to understand protein aggregation and predict amyloid conformation. *Curr. Opin. Struct. Biol.* 10:445–452.
25. Ma, B., and R. Nussinov. 2002. Molecular dynamics simulations of alanine rich β-sheet oligomers: insight into amyloid formation. *Protein Sci.* 11:2335–2350.
26. Cecchini, M., F. Rao, M. Seeber, and A. Caflisch. 2004. Replica exchange molecular dynamics simulations of amyloid peptide aggregation. *J. Chem. Phys.* 121:10748–10756.
27. Wu, C., H. Lei, and Y. Duan. 2005. Elongation of ordered peptide aggregate of an amyloidogenic hexapeptide NFGAIL observed in molecular dynamics simulations with explicit solvent. *J. Am. Chem. Soc.* 127:13530–13537.
28. Nguyen, P. H., M. S. Li, G. Stock, J. E. Straub, and D. Thirumalai. 2007. Monomer adds to preformed structured oligomers of Aβ-peptides by a two-stage dock-lock mechanism. *Proc. Natl. Acad. Sci. USA*. 104:111–116.
29. Krone, M. G., L. Hua, P. Soto, R. Zhou, B. J. Berne, et al. 2008. Role of water in mediating the assembly of Alzheimer amyloid-β Aβ_{16-22} protofilaments. *J. Am. Chem. Soc.* 130:11066–11072.
30. Takeda, T., and D. K. Klimov. 2009. Replica exchange simulations of the thermodynamics of Aβ fibril growth. *Biophys. J.* 96:442–452.
31. Baumketner, A., and J.-E. Shea. 2007. The structure of Alzheimer amyloid β_{10-35} peptide probed through replica exchange molecular dynamics simulations in explicit solvent. *J. Mol. Biol.* 366:275–285.
32. Yang, M., and D. B. Teplow. 2008. Amyloid β-protein monomer folding: free energy surfaces reveal alloform specific differences. *J. Mol. Biol.* 384:450–464.
33. Sgourakis, N. G., Y. Yan, S. A. McCallum, C. Wang, and A. E. Garcia. 2007. The Alzheimers peptides Aβ40 and 42 adopt distinct conformations in water: a combined MD/NMR study. *J. Mol. Biol.* 368:1448–1457.
34. Takeda, T., and D. K. Klimov. 2009. Probing the effect of amino-terminal truncation for Aβ_{1-40} peptides. *J. Phys. Chem. B*. 113:6692–6702.
35. Buchete, N.-V., and G. Hummer. 2007. Structure and dynamics of parallel β-sheets, hydrophobic core, and loops in Alzheimer's Aβ fibrils. *Biophys. J.* 92:3032–3039.
36. Buchete, N.-V., R. Tycko, and G. Hummer. 2005. Molecular dynamics simulations of Alzheimers β-amyloid protofilaments. *J. Mol. Biol.* 353:804–821.
37. Zheng, J., H. Jang, B. Ma, C.-J. Tsai, and R. Nussinov. 2007. Modeling the Alzheimer Aβ_{17-42} fibril architecture: tight intermolecular sheet-sheet association and intramolecular hydrated cavities. *Biophys. J.* 93:3046–3057.
38. Zheng, J., H. Jang, B. Ma, and R. Nussinov. 2008. Annular structures as intermediates in fibril formation of Alzheimer Aβ_{17-42}. *J. Phys. Chem. B*. 112:6856–6865.
39. Wu, C., Z. Wang, H. Lei, Y. Duan, M. T. Bowers, et al. 2008. The binding of thioflavin T and its neutral analog BTA-1 to protofibrils of the Alzheimer's disease Aβ_{16-22} peptide probed by molecular dynamics simulations. *J. Mol. Biol.* 384:718–729.
40. Convertino, M., R. Pellarin, M. Catto, A. Carotti, and A. Caflisch. 2009. 9,10-Anthraquinone hinders β-aggregation: How does a small molecule interfere with Aβ-peptide amyloid fibrillation? *Protein Sci.* 18:792–800.
41. Sugita, Y., and Y. Okamoto. 1999. Replica-exchange molecular dynamics method for protein folding. *Chem. Phys. Lett.* 114:141–151.
42. Brooks, B. R., R. E. Bruccoler, B. D. Olafson, D. J. States, S. Swaminathan, et al. 1982. CHARMM: a program for macromolecular energy, minimization, and dynamics calculations. *J. Comput. Chem.* 4:187–217.
43. Ferrara, P., J. Apostolakis, and A. Caflisch. 2002. Evaluation of a fast implicit solvent model for molecular dynamics simulations. *Proteins*. 46:24–33.
44. Takeda, T., and D. K. Klimov. 2009. Probing energetics of Aβ fibril elongation by molecular dynamics simulations. *Biophys. J.* 96:4428–4437.
45. Takeda, T., and D. K. Klimov. 2009. Interpeptide interactions induce helix to strand structural transition in Aβ peptides. *Proteins*. 77:1–13.
46. Garcia, A. E., and J. N. Onuchic. 2003. Folding a protein in a computer: an atomic description of the folding/unfolding of protein A. *Proc. Natl. Acad. Sci. USA*. 100:13898–13903.
47. Tsai, H.-H., M. Reches, C.-J. Tsai, K. Gunasekaran, E. Gazit, et al. 2005. Energy landscape of amyloidogenic peptide oligomerization by parallel-tempering molecular dynamics simulation: significant role of Asn ladder. *Proc. Natl. Acad. Sci. USA*. 102:8174–8179.

48. Baumketner, A., and J.-E. Shea. 2006. Folding landscapes of the Alzheimer amyloid-β(12–28) peptide. *J. Mol. Biol.* 362:567–579.

49. Jang, S., and S. Shin. 2008. Computational study on the structural diversity of amyloid β peptide ($A\beta_{10-35}$) oligomers. *J. Phys. Chem. B.* 112:3479–3484.

50. Klimov, D. K., and D. Thirumalai. 2003. Dissecting the assembly of $A\beta_{16-22}$ amyloid peptides into antiparallel β-sheets. *Structure.* 11:295–307.

51. Kabsch, W., and C. Sander. 1983. Dictionary of protein secondary structure: pattern recognition of hydrogen-bonded and geometrical features. *Biopolymers.* 22:2577–2637.

52. Ferrenberg, A. M., and R. H. Swendsen. 1989. Optimized Monte Carlo data analysis. *Phys. Rev. Lett.* 63:1195–1198.

53. Vueba, M. L., M. E. Pina, and L. A. E. B. Carvalho. 2008. Conformational stability of ibuprofen: assessed by DFT calculations and optical vibrational spectroscopy. *J. Pharm. Sci.* 97:845–859.

54. Agdeppa, E., V. Kepe, J. Liu, S. Flores-Torres, N. Satyamurthy, et al. 2001. Binding characteristics of radiofluorinated 6-dialkylamino-2-naphthylethylidene derivatives as positron emission tomography imaging probes for β-amyloid plaques in Alzheimers disease. *J. Neurosci.* 21:1–5.

55. Hirohata, M., K. Ono, A. Morinaga, and M. Yamada. 2008. Non-steroidal anti-inflammatory drugs have potent anti-fibrillogenic and fibril-destabilizing effects for α-synuclein fibrils in vitro. *Neuropharmacology.* 54:620–627.

56. Ma, X., L. Liu, X. Mao, L. Niu, K. Deng, et al. 2009. Amyloid β(1–42) folding multiplicity and single-molecule binding behavior studied with STM. *J. Mol. Biol.* 388:894–901.

57. Esler, W. P., E. R. Stimson, J. M. Jennings, H. V. Vinters, J. R. Ghilardi, et al. 2000. Alzheimer's disease amyloid propagation by a template-dependent dock-lock mechanism. *Biochemistry.* 39:6288–6295.

58. Cannon, M. J., A. D. Williams, R. Wetzel, and D. G. Myszka. 2004. Kinetic analysis of β-amyloid fibril elongation. *Anal. Biochem.* 328:67–75.

59. O'Nuallain, B., S. Shivaprasad, I. Kheterpal, and R. Wetzel. 2005. Thermodynamics of Aβ(1–40) amyloid fibril elongation. *Biochemistry.* 44:12709–12718.

60. Ban, T., M. Hoshino, S. Takahashi, D. Hamada, K. Hasegawa, et al. 2004. Direct observation of Aβ amyloid fibril growth and inhibition. *J. Mol. Biol.* 344:757–767.

61. Kellermayer, M. S. Z., A. Karsai, M. Benke, K. Soos, and B. Penke. 2008. Stepwise dynamics of epitaxially growing single amyloid fibrils. *Proc. Natl. Acad. Sci. USA.* 105:141–144.

62. Pettersen, E. F., T. D. Goddard, C. C. Huang, G. S. Couch, D. M. Greenblatt, et al. 2004. UCSF Chimera: a visualization system for exploratory research and analysis. *J. Comput. Chem.* 25:1605–1612.

63. Bathelt, C. M., J. Zurek, A. J. Mulholland, and J. N. Harvey. 2005. Electronic structure of compound I in human isoforms of cytochrome P450 from QM/MM modeling. *J. Am. Chem. Soc.* 127:12900–12908.